

rare-earth carbides and extended it to encompass the tetracarbides. Kohl and Stearns^{31,32} have found this analogy to be applicable to all group 3B and 4B transition-metal di- and tetracarbides. The energy difference between the M–O and M–C₂ bonds may be interpreted as arising from a difference in electronegativity of O and C₂ radicals of 3.5 and 3.3, respectively, on the Pauling scale.¹³

The authors in another paper^{5b} have extended these empirical correlations to a more general explanation of the structures of CeC_n(g) molecules. The significant stability of the C₂ negative ion compared to negative ions of higher carbon chains is supported by molecular orbital considerations.^{34,35} Thus a structure that contains only two small carbon fragments may be a strong possibility as a preferred structure of the numerous Ce₂C_n gaseous molecules. Our evidence for this assumption is very marginal. The only certainty that can be said about these molecules is that the metal atoms are not bonded together.

- (29) Balducci, G.; Calpalbi, A.; DeMaria, G.; Guido, M. *J. Chem. Phys.* **1966**, *43*, 2136; **1969**, *51*, 2871.
 (30) Balducci, G.; DeMaria, G.; Guido, M. "Proceeding of the First International Conference on Calorimetry and Thermodynamics"; Polish Scientific Publ.: Warsaw, 1970; pp 415-421.
 (31) Kohl, F. J.; Stearns, C. A. *J. Chem. Phys.*, **1969**, *52*, 6310. **1971**, *54*, 1414. **1971**, *54*, 5180.
 (32) Kohl, F. J.; Stearns, C. A. *J. Phys. Chem.* **1970**, *74*, 2714. *High Temp. Sci.* **1974**, *6*, 284.
 (33) Gingerich, K. A. *Chem. Phys. Lett.* **1978**, *59*, 136.
 (34) Pitzer, K. S.; Clementi, E. *J. Am. Chem. Soc.* **1959**, *81*, 4477.
 (35) Strickler, S. J.; Pitzer, K. S. In "Molecular Orbitals in Chemistry, Physics, and Biology"; Pullman, B., Löwdin, P.-O., Eds.; Academic Press: New York, 1964; pp 281-292.
 (36) Gupta, S. K.; Kingcade Jr., J. E.; Gingerich, K. A. *Adv. Mass Spectrom.* **1980**, *8*, 445.

The latter statement can be supported by the difference $\Delta H_a^\circ(Ce_2C_n) - \Delta H_a^\circ(CeC_n)$, Table IV. This difference represents the bond dissociation of the second cerium metal atom. The value of the difference increases with increasing C_n size (except in the case of Ce₂C). These values are approximately equal to the corresponding bond dissociation of the monocerium carbides, CeC_n.

Also the difference $\Delta H^\circ_0(Ce_2C_n) - \Delta H^\circ_0(C_n)$, which is approximately 1200 kJ mol⁻¹, is significantly higher than the reported dissociation energy of Ce₂, $D^\circ_0 = 238 \pm 21$ kJ mol⁻¹,³ thereby implying strongly that the Ce–Ce bond is not contained within the molecule.

The results and discussion presented in the present paper amply demonstrate the very complex nature of the vapors of transition-metal carbides. If a stable dicarbide exists [D°_0 -(M–C₂) 600 kJ mol⁻¹], one will observe a whole series of species of the types MC_n and M₂C_n at high enough temperatures. While we have suggested choices in predicting structures, there is very little information available with which to accurately estimate the various partition functions. Therefore we hope that this discussion will stimulate theoretical and optical spectroscopic investigations that can be expected to enhance the knowledge of the molecular and electronic structure and of the nature of bonding in these types of molecules.

Acknowledgment. This work has been generously supported by the National Science Foundation under Grant CHE-8007549.

Registry No. Ce, 7440-45-1; Ce₂C, 58591-86-9; Ce₂C₂, 12011-58-4; Ce₂C₃, 12115-63-8; Ce₂C₄, 12012-32-7; Ce₂C₅, 58591-83-6; Ce₂C₆, 39461-15-9; graphite, 7782-42-5.

Contribution from the Department of Chemistry, Washington State University, Pullman, Washington 99164-4630

Electron Self-Exchange by Hexakis(cyclohexyl isocyanide)manganese(I/II): Solvent, Electrolyte, and Temperature Dependences¹

ROGER M. NIELSON and SCOT WHERLAND*

Received July 18, 1983

The rate of electron self-exchange between MnL₆BF₄ and MnL₆(BF₄)₂ (L is CNC₆H₁₁) has been measured by ⁵⁵Mn NMR line broadening as a function of reactant concentration, solvent, added electrolyte, and temperature. Ion association between the manganese complexes and BF₄⁻ has been measured by conductivity. The second-order rate constants at 26 °C and the activation parameters in the presence of 0.08 M tetrabutylammonium tetrafluoroborate are as follows (10⁻⁵k in M⁻¹s⁻¹, ΔH^\ddagger in kcal/mol, ΔS^\ddagger in cal/(mol deg)): dimethyl sulfoxide, 10.8 ± 0.6, 3.5 ± 1.5, -19 ± 5; acetonitrile, 4.38 ± 0.07, 3.4 ± 0.1, -21 ± 1; ethanol, 2.51 ± 0.02, 3.5 ± 0.1, -22 ± 1; acetone, 2.51 ± 0.04, 3.5 ± 0.1, -22 ± 1; bromobenzene, 0.961 ± 0.001, 6.0 ± 0.1, 15 ± 1; chloroform, 0.585 ± 0.006, 4.3 ± 0.1, -22 ± 1. The dependence of the rate constants on added electrolyte varied with the solvent, increasing with added salt in the more polar solvents and decreasing in the less polar solvents. This has been interpreted in terms of electrostatic work in forming the precursor complex and inhibition by ion association. The rate constants for the various paths in the different solvents have been resolved by using the kinetic and conductivity data. The solvent dependence of these rate constants is opposite in sign to that predicted, by using dielectric continuum theory for the solvent reorganization, within Marcus' theory for outer-sphere electron transfer.

Introduction

Recent research activity in the field of electron-transfer reactions has involved refinement of the theoretical models and extension and refinement of experimental measurements in a cooperative manner.²⁻⁵ This has led to significant progress

in an area that has long been an active one. In our laboratory we are pursuing detailed studies of well-defined outer-sphere electron-transfer systems in order to assess the influence of solvent, ion pairing, and variation of the size of the complexes on electron-transfer efficiency and to compare the results with the predictions of current theories.^{6,7} Relatively little work has been done on electron transfer by substitution-inert transition-metal complexes in nonaqueous solvents, but those

- (1) Presented in part at the 185th National Meeting of the American Chemical Society Seattle, WA, March 1983.
 (2) Cannon, R. D. "Electron Transfer Reactions"; Butterworths: London, 1980.
 (3) Tembe, B. L.; Friedman, H. L.; Newton, M. D. *J. Chem. Phys.* **1982**, *76*, 1490.
 (4) Sutin, N. *Acc. Chem. Res.* **1982**, *15*, 275.

- (5) Sutin, N. In "Inorganic Biochemistry"; Eichorn, G. L., Elsevier: New York, 1973; Vol. 2, pp 611-53.
 (6) Borchardt, D.; Pool, K.; Wherland, S. *Inorg. Chem.* **1982**, *21*, 93.
 (7) Borchardt, D.; Wherland, S. *Inorg. Chem.*, in press.

studies that have been done are starting to show a sizable effect from the ion pairing that necessarily occurs in low-dielectric solvents and also show in several cases that the solvent effect cannot be predicted well by dielectric-continuum theories.⁷⁻¹⁰ The question of the effect of complex size and electron-transfer distance on the efficiency of bimolecular electron transfer is a challenging one for the experimentalist. The theory, which must consider changes in the importance of electron or nuclear tunneling in the process, is currently being vigorously debated.¹¹ Detailed experiments that vary the electron-transfer distance and as little more than that as possible, while monitoring effects of size on solvation, ion pairing, and the work required to bring the reactants together, are needed.

The system we have chosen for detailed study is the family of manganese(I) and manganese(II) hexakis(alkyl isocyanide) complexes. These complexes are substitution inert, and the electron self-exchange can be followed directly by NMR line-broadening methods; the alkyl group and thus the electron-transfer distance can be varied without changing the electronic properties of the metal center, and the complexes are soluble in a variety of solvents.¹² It is especially important that the self-exchange rates can be measured directly, since this is the parameter most easily treated by electron-transfer theory. In this first paper from our laboratory on these reactions, we present studies of the reactivity of hexakis(cyclohexyl isocyanide) complexes as a function of reactant concentration, solvent, added electrolyte, and temperature, as well as conductivity studies to establish the ion-association constants. By measuring the rate constants for the various ion-paired species independently, we can properly test the theoretical prediction of the solvent dependence. This work sets the reference point for further studies in which other alkyl groups are being studied and activation volumes are going to be measured as a method of approaching experimentally the contribution of solvation to the electron-transfer process.

Experimental Section

Cyclohexyl isocyanide was prepared according to a literature method,¹³ except that benzenesulfonyl chloride was used as the dehydrating agent. Manganese(II) iodide was prepared by adding a stoichiometric amount of fresh 47–51% hydriodic acid (Baker) to a stirred solution of manganese(II) carbonate in ethanol. Drying under vacuum gave the desired product.

Hexakis(cyclohexyl isocyanide)manganese(I) iodide ($(\text{C}_6\text{H}_{11}\text{N}-\text{C})_6\text{MnI}$) was made by the method of Sacco¹⁴ except that the reaction was run at room temperature, no iodine was added, and the reductant was sodium thiosulfate instead of sodium dithionite. The analogous tetrafluoroborate salt was made by dissolving the iodide salt in ethanol and adding an equimolar amount of silver tetrafluoroborate. The resulting silver iodide was filtered off, and the complex was precipitated by the addition of water. The $(\text{C}_6\text{H}_{11}\text{NC})_6\text{MnBF}_4$ was recrystallized five times from hot ethanol–water; mp 152–154 °C. Anal. Calcd: C, 63.39; H, 8.36; N, 10.56. Found: C, 63.38; H, 8.40, N, 10.60. Microanalysis was done by Canadian Microanalytical.

Hexakis(cyclohexyl isocyanide)manganese(II) tetrafluoroborate ($(\text{C}_6\text{H}_{11}\text{NC})_6\text{Mn}(\text{BF}_4)_2$) was prepared according to the method of Bailey¹⁵ except that equimolar nitric acid was used as the oxidant and fluoboric acid was used as the anion source. The complex was recrystallized three times from acetone–water without heating; mp 98 °C dec. Anal. Calcd: C, 57.14; H, 7.54; N, 9.52. Found: C, 56.84; H, 7.67; N, 9.41.

All solvents were reagent grade and were purified by literature methods¹⁶ and used immediately after purification. Distillation was through a 70-cm Vigreux column, and the middle 70% was used. Dimethyl sulfoxide (Baker) was stirred with Drierite for 2 days, with a fresh portion of the desiccant added after 24 h, and vacuum distilled from fresh Drierite. Acetone was prepared similarly, except that vacuum distillation was not required. Acetonitrile was refluxed for 24 h over phosphorus pentoxide and fractionally distilled at atmospheric pressure. USP grade ethanol (USI) was purified by the procedure Lund and Bjerrum¹⁷ developed for methanol. Bromobenzene (Aldrich) was vacuum distilled from Drierite. Chloroform was washed once with dilute sodium hydroxide and five times with water. It was then dried overnight in the dark with Drierite and distilled.

The electrolyte tetrabutylammonium tetrafluoroborate (Bu_4NBF_4) was prepared from tetra-*n*-butylammonium bromide (Aldrich) and fluoboric acid (Baker) and recrystallized repeatedly from ethyl acetate and diethyl ether after thorough drying.

The cell used for the conductivity experiments had a cell constant of 0.7810 cm^{-1} and a volume of 60 mL. The cell constant was measured by using aqueous KCl solutions. Temperature was maintained at 26 ± 0.02 °C with a Forma circulating bath and a Sargent Thermonitor proportional controller regulating heater in a rapidly stirred 8-L mineral oil bath. Conductance measurements were made with an Industrial Instruments RC-18 bridge in parallel to a 1000- Ω resistor. The resistance of this resistor was checked for each measurement of the cell.

A Nicolet NT200WB instrument with quadrature-phase detection operating at 49.52 MHz was used for all NMR data collection. Spectra were measured over a 6024-Hz width. Data acquisition was by a single-pulse technique with a pulse width of 20 μs and an 83- μs delay before the beginning of data collection. The acquired block size was typically 4096 points for solutions of only the Mn(I) complex and down to 512 points for solutions with added Mn(II) complex. A 0.5- μs delay after data acquisition was used. Under these conditions, a good signal-to-noise ratio could be attained in a few minutes by collecting 2500–10 000 pulses. Line widths were not significantly decreased by spinning the sample.

Temperature was controlled with the built-in gas-flow temperature controller. This system, using dry nitrogen flowing through a coil immersed in liquid nitrogen, could give a minimum temperature of about –45 °C. The accuracy of the control was checked with a thermocouple immersed in a solvent in a sample tube. Samples could not be spun for this measurement and thus were not spun for the spectral measurements. The range of temperatures used was dictated by this low-temperature limit of the spectrometer, the freezing point of the solvents, decomposition of the samples at temperatures much above 26 °C, and the lack of broadening observed at lower temperatures in some of the solvents. The temperature ranges that could be used were –35 to 26 °C for acetonitrile, ethanol, and acetone, –30 to +26 °C for bromobenzene, –25 to +26 °C for chloroform, and 15–30 °C for dimethyl sulfoxide.

The complexes were stored over dry ice, where they were stable for weeks, as indicated by the line-broadening experiments and by cyclic voltammetry measurements. The solids were allowed to come to room temperature in a desiccator, weighed, and then kept in dry ice until the solvent was added and the spectra were measured. All measurements were done within 30 min of adding the solvent. The stability of the solutions was checked by measuring the line widths at various time intervals. Solutions of the Mn(I) complex were stable for days in all solvents. The solutions of Mn(I) and Mn(II) complexes were stable for 2 h in acetone and dimethyl sulfoxide and for 8 h in the other solvents.

The frequency-domain NMR data were fit to a Lorentzian line shape by using a least-squares-minimizing program available on the Nicolet instrument. Typically, 50–90 points above the base line were used in the fitting.

The fitting of the conductivity data and the rate equations was done by least-squares techniques, using the reciprocal of the variance as the weighting factor, on a Cromemco Z80 based system using Fortran. Least-squares programs were based on those of Bevington.¹⁸

- (8) Yang, E. S.; Chau, M. S.; Wahl, A. C. *J. Phys. Chem.* **1980**, *84*, 3094.
- (9) Chau, M.-S.; Wahl, A. C. *J. Phys. Chem.* **1982**, *86*, 126.
- (10) Tomi, T. T.; Weaver, M. J.; Brubaker, C. H., Jr. *J. Am. Chem. Soc.* **1982**, *104*, 2381.
- (11) Chance, B.; DeVault, D. C.; Frauenfelder, H.; Marcus, R. A.; Schrieffer, J. R.; Sutin, N., Eds. "Tunnelling in Biological Systems"; Academic Press: New York, 1979.
- (12) Matteson, D. S.; Bailey, R. J. *Am. Chem. Soc.* **1969**, *91*, 1975.
- (13) Ugi, I.; Meyer, R.; Lipinski, M.; Bodesheim, F.; Rosendahl, F. *Org. Synth.* **1961**, *41*, 3.
- (14) Sacco, I. *Ann. Chim. (Rome)* **1958**, *48*, 225.
- (15) Bailey, R. A. Ph.D. Thesis, Washington State University, 1968.

- (16) Riddick, J. A.; Bunger, W. B. "Organic Solvents: Physical Properties and Methods of Purification", 3rd ed.; Wiley: New York, 1970.
- (17) Lund, H.; Bjerrum, J. *Ber. Dtsch. Chem. Ges. A* **1931**, *64*, 210.
- (18) Bevington, P. E. "Data Reduction and Error Analysis for the Physical Sciences"; McGraw-Hill: New York, 1969.

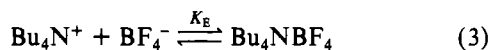
Table I. Association Constants from Conductivity at 26 °C

| complex | solvent ^a | $K_{1,2}$ | K^b | Λ_{∞}^c , $\Omega^{-1} \text{ cm}^{-1}$ | r , Å | concn, mM |
|--|---------------------------------|------------------------------|-------------------|---|---------|-----------------|
| $(\text{C}_6\text{H}_{11}\text{NC})_6\text{MnBF}_4^-$ | $(\text{CH}_3)_2\text{SO}$ | small ^c | 1×10 | | 11 | |
| | CH_3CN | 1×10^{-4} | 1.3×10 | 153.0 | 7 | 0.1323–2.646 |
| | $\text{C}_2\text{H}_5\text{OH}$ | 4×10 | 2.6×10 | 46.5 | 15 | 0.075 05–1.500 |
| | $(\text{CH}_3)_2\text{CO}$ | 2×10 | 3.9×10 | 166.1 | 11 | 0.007 500–1.007 |
| | $\text{C}_6\text{H}_5\text{Br}$ | 8×10^4 | 4.0×10^5 | 34.6 | 27 | 0.043 98–1.309 |
| | CHCl_3 | 7×10^4 | 1.3×10^5 | 46.7 | 34 | 0.050 07–1.255 |
| $(\text{C}_6\text{H}_{11}\text{NC})_6\text{Mn}(\text{BF}_4)_2$ | $(\text{CH}_3)_2\text{SO}$ | small ^c | 3×10 | | 11 | |
| | CH_3CN | small ^c | 5×10 | | 11 | |
| | $\text{C}_2\text{H}_5\text{OH}$ | 1×10^4 ^e | 2×10^2 | 54.0 | 11 | 0.022 71–0.4541 |
| | $(\text{CH}_3)_2\text{CO}$ | 2×10^2 ^e | 5×10^2 | 203.1 | 11 | 0.023 07–0.4614 |
| | $\text{C}_6\text{H}_5\text{Br}$ | large ^d | 5×10^8 | | 11 | |
| | CHCl_3 | large ^d | 5×10^9 | | 11 | |
| $[\text{CH}_3(\text{CH}_2)_3]_4\text{NBF}_4^-$ | $(\text{CH}_3)_2\text{SO}$ | 3 | 4 | 37.6 | 16 | 0.1568–3.136 |
| | CH_3CN | 1×10 | 7 | 171.6 | 7 | 0.1234–2.468 |
| | $\text{C}_2\text{H}_5\text{OH}$ | 2.3×10^2 | 2×10 | 51.5 | 8 | 0.1368–2.737 |
| | $(\text{CH}_3)_2\text{CO}$ | 1.3×10^2 | 5×10 | 193.6 | 14 | 0.1231–2.462 |
| | $\text{C}_6\text{H}_5\text{Br}$ | large ^d | 2×10^7 | | 6 | |
| | CHCl_3 | 2×10^7 | 1×10^8 | 12.0 | 7 | 0.024 17–1.209 |

^a Solvent dielectric constants and viscosities (cP): dimethyl sulfoxide, 46.7, 1.96; acetonitrile 37.5, 0.338; ethanol 24.6, 1.08; acetone 20.7, 0.316; bromobenzene 5.40, 0.985; chloroform 4.80, 0.534.¹⁶ ^b Association constant calculated from eq 4. The radius was taken as 11 Å for the manganese complexes and 6 Å for $\text{Bu}_4\text{NBF}_4^-$. ^c Actual values could not be measured because of the small change of conductance with concentration. ^d Actual values not measured; total association assumed. ^e The limiting conductance of BF_4^- was taken as $26 \Omega^{-1} \text{ cm}^{-1}$ in ethanol and $101 \Omega^{-1} \text{ cm}^{-1}$ in acetone.

Results and Calculations

In order to establish the extent of ion pairing (eq 1–3) in the various solvents, the necessary conductivity data were obtained for MnL_6BF_4 (L is $\text{CNC}_6\text{H}_{11}$), $\text{MnL}_6(\text{BF}_4)_2$, and Bu_4NBF_4 . The conductivity data are collected in Table A,



and an example of a conductance vs. concentration plot is shown in Figure A. (The lettered tables and figures are available as supplementary material.) The data for the one-to-one electrolytes were fit to the equations of Fuoss and Hsia¹⁹ in the form presented by Fernandez-Prini.²⁰ Following the suggestions of Beronius,²¹ only the limiting conductance and the association constant were treated as adjustable parameters in the computer-fitting program, and the radius parameter of the theory was optimized by setting it equal to a variety of values and optimizing the other two parameters until a minimum in χ^2 was obtained. The measurements were of comparable precision, and unit weights were used. The results of these fits are shown in Table I along with the values of the constants needed and the concentration range of the data used. For the Mn(II) complex the method of Fuoss and Edelson²² was used, as has previously been applied by Petrucci and co-workers²³ and by Libus et al.²⁴ In this method it is assumed that only the equilibrium in eq 2 is being observed. A value must be assumed for the limiting conductance of the BF_4^- ion, and the ion pair $\text{MnL}_6\text{BF}_4^+$ was assumed to have a limiting conductance half that of the MnL_6^{2+} ion. The association constant was not sensitive to moderate changes in these assumptions. The theory is valid only for data at low concentrations which give a linear fit to the Fuoss and Edelson equation, so trial plots were made of the data, and only the

linear part of the curves was used for evaluation of the constants. The results of these analyses are in Table I along with the values of the parameters used.

The ion-association constants derived in the analysis of the conductivity data are for the limit of infinite dilution and thus unit activity. They can be compared to approximate values calculated from eq 4,²⁵ which have been rewritten for the case

$$K = \frac{4\pi N r^3}{3 \times 10^3} \exp(-w/RT) \quad (4a)$$

$$w = \frac{Z_1 Z_2 e^2}{\epsilon r} \quad (4b)$$

of zero ionic strength in esu units. In these equations, N is Avogadro's number, r is conventionally taken as the distance between the centers of the two ions involved in the ion pair, R is the gas constant, T is the absolute temperature, Z_1 and Z_2 are the charges on the two ions, e is the charge on the electron, and ϵ is the dielectric constant. The comparisons with these estimates are in Table I.

In order to calculate the concentrations of the various species present under the conditions used in the experiments, an expression for the activity coefficients must be selected. We used eq 5a–c, which are consistent with those used in the conduc-

$$-\ln \gamma = \frac{Z^2 C \mu^{1/2}}{1 + B a \mu^{1/2}} \quad (5a)$$

$$C = \left(\frac{2\pi N}{1000} \right)^{1/2} \left(\frac{e^2}{\epsilon k_B T} \right)^{3/2} \quad (5b)$$

$$B = \left(\frac{8\pi N e^2}{1000 \epsilon k_B T} \right)^{1/2} \quad (5c)$$

tivity equations. In eq 5c, the symbols not previously defined are k_B , the Boltzmann constant, a , the distance of closest approach between an ion and its counterions, and μ , the ionic strength of the medium. By use of eq 5 and the association constants, the concentration of all species can be calculated by first assuming unit activities and calculating the concentration of all ions and the ionic strength of the medium and then recalculating the activity coefficients and repeating the

(19) Fuoss, R. M.; Hsia, K.-L. *Proc. Natl. Acad. Sci. U.S.A.* **1967**, *59*, 1550.

(20) Fernandez-Prini, R. *Trans. Faraday Soc.* **1969**, *65*, 3311.

(21) Beronius, P. *Acta. Chem. Scan. Ser. A* **1975**, *A29*, 289.

(22) Fuoss, R. M.; Edelson, D. *J. Am. Chem. Soc.* **1951**, *73*, 269.

(23) Diamond, A.; Fanelli, A.; Petrucci, S. *Inorg. Chem.* **1973**, *12*, 611.

(24) Libus, W.; Chachulski, B.; Frazczyk, L. *J. Solution Chem.* **1980**, *9*, 355.

(25) Brown, G. M.; Sutin, N. *J. Am. Chem. Soc.* **1979**, *101*, 883.

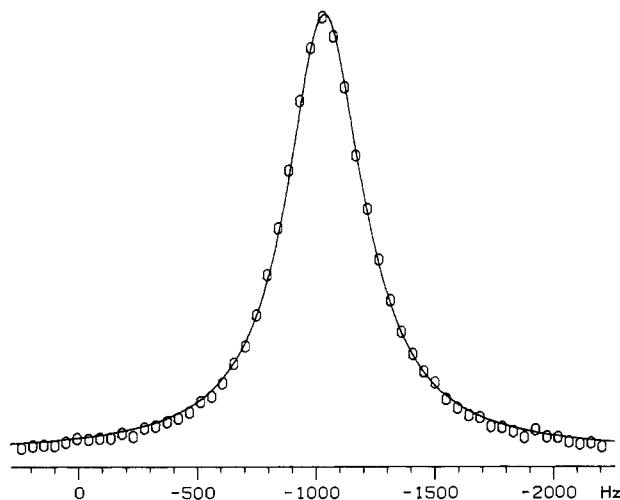


Figure 1. ^{55}Mn NMR line shape. Solid line is the fit to a Lorentzian line shape. Circles are the actual data points. $\Delta\nu = 396.8 \text{ Hz} \pm 2.9$. Number of data points = 59.

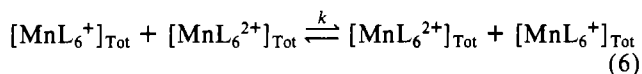
Table II. Observed Second-Order Rate Constants and Activation Parameters at 26 °C and 0.08 M Added Bu_4NBF_4

| solvent | $10^{-5}k(\text{obsd}), \text{M}^{-1} \text{s}^{-1}$ | $\Delta H^\ddagger, \text{kcal mol}^{-1}$ | $\Delta S^\ddagger, \text{cal mol}^{-1} \text{K}^{-1}$ | temp range, °C |
|---------------------------------|--|---|--|----------------|
| $(\text{CH}_3)_2\text{SO}$ | 10.8 (0.6) ^a | 3.5 (1.5) | -19 (5) | 15-30 |
| CH_3CN | 4.38 (0.07) | 3.4 (0.1) | -21 (1) | -35 to +26 |
| $\text{C}_2\text{H}_5\text{OH}$ | 2.51 (0.02) | 3.5 (0.1) | -22 (1) | -35 to +26 |
| $(\text{CH}_3)_2\text{CO}$ | 2.51 (0.04) | 3.5 (0.1) | -22 (1) | -35 to +26 |
| $\text{C}_6\text{H}_5\text{Br}$ | 0.961 (0.001) | 6.0 (0.1) | -15 (1) | -30 to +26 |
| CHCl_3 | 0.585 (0.006) | 4.3 (0.1) | -22 (1) | -25 to +26 |

^a Estimated errors in parentheses.

process until a consistent set of concentrations and ionic strength is obtained. In this procedure it was assumed that the $\text{MnL}_6\text{BF}_4^+$ ion had the same association constant with fluoborate as did the MnL_6^+ ion.

The rate of the electron-self-exchange process, eq 6, where the subscript "Tot" refers to all forms of the particular oxidation state, was obtained from ^{55}Mn NMR line width measurements by the method of Matteson and Bailey.¹² The effect



of the electron transfer is to shorten the apparent spin-spin (T_2) relaxation time of the diamagnetic $\text{Mn}(\text{I})$ complex. Assuming this mechanism, eq 7 holds where T_{2P} is for the

$$k = ([\text{MnL}_6^{2+}]_{\text{Tot}})^{-1}((1/T_{2P}) - (1/T_{2D})) \quad (7a)$$

$$1/T_2 = \pi\Delta\nu \quad (7b)$$

mixture of $\text{Mn}(\text{I})$ and $\text{Mn}(\text{II})$ complexes, T_{2D} is for the $\text{Mn}(\text{I})$ complex alone, and the $\Delta\nu$ is the full width at half-height of the observed line. Figure 1 shows an example of the data obtained and the fit to a Lorentzian line shape. Adherence to the prediction of eq 7 is shown in Figure 2, which is a plot of $1/T_2$ of the ^{55}Mn resonance vs. the concentration of added paramagnetic $\text{Mn}(\text{II})$ complex for each solvent. Table II shows the apparent second-order rate constants for the dependence on the $\text{Mn}(\text{II})$ complex concentration at 26 °C and 0.08 M Bu_4NBF_4 .

Supplementary Table B contains the NMR data, including the experimental conditions of solvent, temperature, reactant, and electrolyte concentrations, for each experiment. Also included are the rate constants calculated for each sample, on the basis of eq 7, and the standard deviations associated with these values.

The Eyring plots of the temperature dependence data are shown in Figure 3, and the parameters from the fits to all of

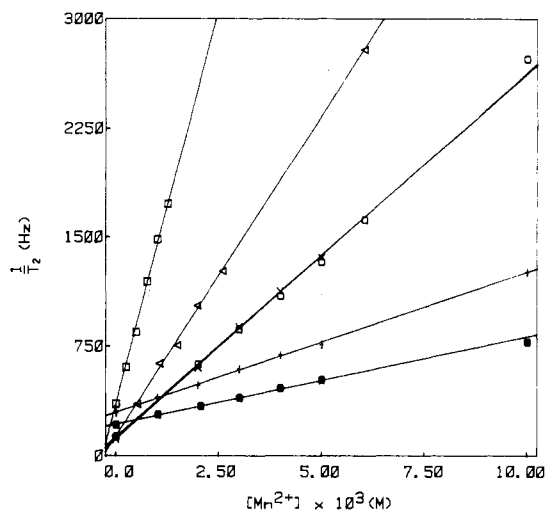


Figure 2. Dependence of $1/T_2$ on the $(\text{C}_6\text{H}_{11}\text{NC})_6\text{Mn}(\text{BF}_4)_2$ concentration at 26 °C in different solvents ($[(\text{C}_6\text{H}_{11}\text{NC})_6\text{MnBF}_4] = 0.02 \text{ M}$, $[\text{Bu}_4\text{NBF}_4] = 0.08 \text{ M}$): (\square) $(\text{CH}_3)_2\text{SO}$; (Δ) CH_3CN ; (\circ) $\text{C}_2\text{H}_5\text{OH}$; (\times) $(\text{CH}_3)_2\text{CO}$; ($+$) $\text{C}_6\text{H}_5\text{Br}$; (\bullet) CHCl_3 .

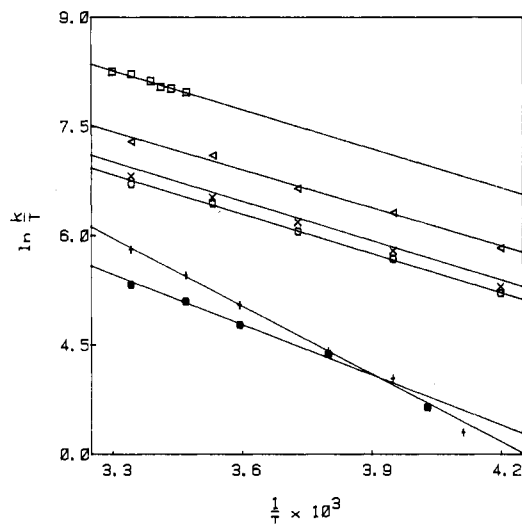


Figure 3. Eyring plots of the temperature dependences in different solvents ($[\text{Bu}_4\text{NBF}_4] = 0.08 \text{ M}$): (\square) $(\text{CH}_3)_2\text{SO}$; (Δ) CH_3CN ; (\circ) $\text{C}_2\text{H}_5\text{OH}$; (\times) $(\text{CH}_3)_2\text{CO}$; ($+$) $\text{C}_6\text{H}_5\text{Br}$; (\bullet) CHCl_3 .

the temperature dependences are set out in Table II.

The effect of added Bu_4NBF_4 varies in magnitude and direction with the solvent. The results are displayed in Figure 4 with the rate normalized for the $\text{Mn}(\text{II})$ and $\text{Mn}(\text{I})$ complex concentrations and plotted against the total BF_4^- concentration from all sources. Each point is calculated from one T_{2P} and the associated T_{2D} measurement, assuming adherence to eq 7.

Discussion

The association constants in Table I are in reasonable agreement with the predictions of eq 4, but the variation from the predicted values shows the necessity of direct measurements. By the use of these association constants and the calculations described above, it can be shown that only totally dissociated electrolytes exist in significant concentration and are involved in the electron self-exchange in dimethyl sulfoxide and acetonitrile over the range of reactant and electrolyte concentrations studied. The same calculations show that in bromobenzene and chloroform the salts do not dissociate appreciably. In ethanol and acetone the extent of ion pairing varies with added Bu_4NBF_4 and with the concentration of the manganese complexes. An example of this is shown in Figure 5, which displays the concentrations of the various species

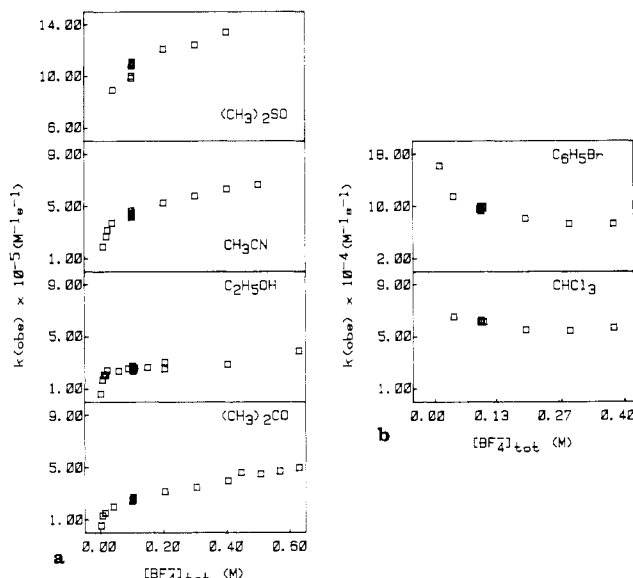


Figure 4. Plots showing the dependence of the normalized rate, k_{obs} , on the total fluoborate concentration from all sources.

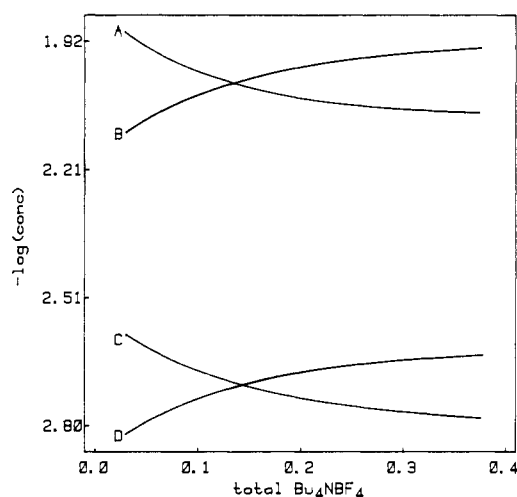
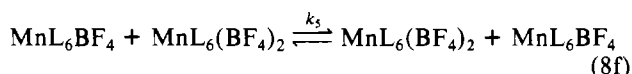
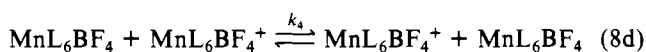
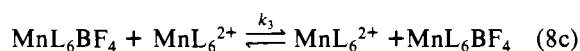
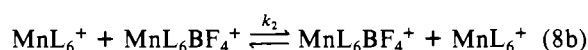


Figure 5. Plots of the $-\log$ of the concentration of the species present in solution vs. the total added Bu_4NBF_4 in $\text{C}_2\text{H}_5\text{OH}$; (A) MnL_6^+ ; (B) MnL_6BF_4 ; (C) $\text{MnL}_6\text{BF}_4^+$; (D) $\text{MnL}_6(\text{BF}_4)_2$. The total concentrations of Mn(I) and Mn(II) species are 0.02 and 0.004 M, respectively.

present in an ethanol solution that is 4.0 mM in the Mn(II) complex, is 2.0 mM in the Mn(I) complex, and has varying amounts of Bu_4NBF_4 . The analysis of the effect of added electrolyte on the reactions must consider the possibility of at least five paths, shown in eq 8a–f. The paths will be referred



to by the subscripts on the rate constants. In all cases the species with varying numbers of fluoborates must be considered

Table III. Second-Order Rate Constants at 26 °C

| solvent | path | $10^{-5}k$, $\text{M}^{-1} \text{s}^{-1}$ | $10^{-5}k_{\text{max}}$, $\text{M}^{-1} \text{s}^{-1}$ | $10^{-5}k_{\text{min}}$, $\text{M}^{-1} \text{s}^{-1}$ |
|-----------------------------------|----------------|---|--|--|
| $(\text{CH}_3)_2\text{SO}$ | 1 ^a | 32 | 35 | 29 |
| CH_3CN | 1 ^a | 13 | 14 | 12 |
| $\text{C}_2\text{H}_5\text{OH}$ | 2 ^a | 10 | 11 | 9 |
| | 5 | 6.7 | 7.6 | 5.8 |
| $(\text{CH}_3)_2\text{CO}$ | 2 ^a | 8.0 | 9.0 | 7.0 |
| | 5 | 18 | 21 | 15 |
| $\text{C}_6\text{H}_5\text{Br}^c$ | 5 | 2.0 | 2.1 | 1.9 |
| | 6 | 0.67 | 0.70 | 0.63 |
| CHCl_3^c | 5 | 0.71 | 0.79 | 0.68 |
| | 6 | 0.52 | 0.54 | 0.49 |

^a In the absence of electrostatic interaction (infinite ionic strength). ^b k_{max} and k_{min} represent the upper and lower limit of k . For the solvents $(\text{CH}_3)_2\text{SO}$, CH_3CN , $\text{C}_2\text{H}_5\text{OH}$, and $(\text{CH}_3)_2\text{CO}$ these values are the standard deviations obtained from the linear least-squares fit. The data in the solvents $\text{C}_6\text{H}_5\text{Br}$ and CHCl_3 were fit to a nonlinear least-squares method and the error was calculated from the method of support planes (Duggleby, R. G. *Eur. J. Biochem.* 1980, 109, 93). ^c The rate law used in fitting the data in these solvents required the equilibrium constant for dipole-dipole association to be fit as a variable parameter. The value of this parameter and the upper and lower limits are as follows: $\text{C}_6\text{H}_5\text{Br}$, 46, 51, 41; CHCl_3 , 13, 31, 7.

as possibly reacting at different rates. In addition, the two paths that involve the reaction between two ions, paths 1 and 2, will be ionic strength dependent. Path 3 is unlikely to be significant in any solvent since it involves the reaction of MnL_6^{2+} ion with MnL_6BF_4 , and in all cases MnL_6^{2+} will form ion pairs at lower concentrations of Bu_4NBF_4 than will MnL_6^+ . The calculated species concentrations support this expectation. Path 4 has two contributions, both of which involve two BF_4^- ions in the transition state and occur with equal probability ($[\text{MnL}_6(\text{BF}_4)_2][\text{MnL}_6^+] = [\text{MnL}_6\text{BF}_4^+][\text{MnL}_6\text{BF}_4]$) on the basis of the concentration of the species. This occurs because of the assumed equivalence of the ion-association constants for the two monocationic manganese complexes.

In order to test this model for the reactions, the calculated species concentrations and rate constants for a given solvent at 26 °C were fit to the rate law with the appropriate paths, assuming a rapid equilibrium for all of the ion association and aggregation steps. For dimethyl sulfoxide and acetonitrile in which only path 1 was operative, the ionic strength dependence was taken into account through the work term in eq 9.^{26,27} In

$$k = A e^{-w/RT} e^{-\Delta G^{**}/RT} \quad (9a)$$

$$w = \frac{Z_1 Z_2 e^2}{\epsilon r} - \frac{Z_1 Z_2 e^2 \beta}{\epsilon(1 + \beta r)} \quad (9b)$$

$$\beta = \text{B}\mu^{1/2} \quad (9c)$$

this equation, A is a frequency factor that is influenced by steric and electronic effects,⁴ and ΔG^{**} is defined below. The approach distance (r) was taken as 11.25 Å for all solvents. These distances are appropriate for the contact distances as estimated from molecular models. This value is different from that derived in the conductivity fits since the distance in the ion-association theory is more closely related to the distance at which the electrostatic interaction between two ions reaches a critical value, and this distance increases rapidly as the dielectric constant decreases. The fit to the rate law using only path 1 has only one adjustable parameter, the rate constant with no electrostatic interaction, or in other words the rate constant predicted at infinite ionic strength if further ion pairs were not formed. This is the rate constant most appropriate

(26) Haim, A.; Sutin, N. *Inorg. Chem.* 1976, 15, 476.

(27) Wherland, S.; Gray, H. B. *Proc. Natl. Acad. Sci. U.S.A.* 1976, 73, 2950.

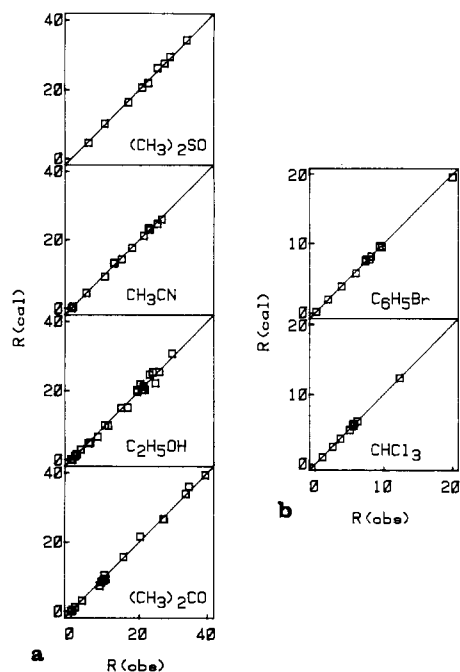
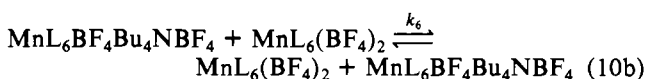


Figure 6. Plots of the calculated rate, R_{cal} , vs. the observed rate, R_{obs} .

for comparison with the other paths for which there is no electrostatic work involved in forming the precursor complex. The results of the fits are given in Table III. Some of the scatter in the plots of the data in Figure 4 is due to the presentation. This occurs since some of the points at a given total BF_4^- concentration are at different ionic strengths owing to different Mn(I) complex and Mn(II) complex concentrations. Figure 6 shows plots of calculated vs. observed rate constants that properly illustrate the precision of the fits.

For the solvents ethanol and acetone, the species distribution calculations showed that paths 2, 4, and 5 could be significant. A multiple linear regression fit was performed, and this showed that the data could be fit well without a contribution from path 4 and that when this path was included, its rate constant was quite poorly defined. The results of the fit are shown in Table III. Again, the quality of the fit is best seen in Figure 6 while the trend with increasing BF_4^- is illustrated in Figure 4.

For the last two solvents, bromobenzene and chloroform, the ion-association constants predict that there should be no change in association over the range studied since the electrolytes are all ion paired. In both cases, however, the rate decreases with added Bu_4NBF_4 . Such behavior has also been observed for the reduction of the clathrochelate $\text{Co}(\text{dmg})_3(\text{BF}_4)_2$ (dmg is the doubly deprotonated dimethylglyoxime ligand) by ferrocene in ethylene dichloride.⁷ The simplest model is to propose additional association between one of the reactants and the added Bu_4NBF_4 . We will write this as association between the dipolar MnL_6NBF_4 ion pair and Bu_4NBF_4 for concreteness, and because this manganese complex is less crowded, probably has a higher dipole moment, and is at a higher concentration than $\text{MnL}_6(\text{BF}_4)_2$. The added equilibrium and kinetic paths are given in eq 10 and the resulting rate law is given in eq 11. A weighted least-squares



$$\text{rate} = \frac{k_5 + k_6 K_3 [\text{Bu}_4\text{NBF}_4]}{1 + K_3 [\text{Bu}_4\text{NBF}_4]} [\text{MnL}_6\text{BF}_4]_{\text{Tot}} [\text{MnL}_6(\text{BF}_4)_2]_{\text{Tot}} \quad (11)$$

fit to this rate law gives the rate constants and association constants in Table III. The equilibrium constants for the associations between the neutral species cannot be estimated as was done for the electrostatic interactions, but they are expected to be much weaker than observed for ion pairing, and this is found.

The excellence of the fits in all cases supports our model for the added salt dependences. For those reactions involving path 1 or 2, the accurate modeling supports the choice for the electrostatic work term function. This also gives us confidence that the extrapolated rate constant derived accurately predicted the rate in the absence of electrostatic work in forming the precursor complex.

The pattern is emerging, although it is not universal, that ion association decreases electron-transfer rates. The only case in the present work in which the more highly associated path does not have a lower rate constant than a less associated path is in acetone. This generalization applies to systems in which there is no electrostatic work required to form the precursor complex or those in which this contribution can be factored out. Endicott and co-workers have recently found systems in which ion pairing by counterions that are involved in charge-transfer interactions with the metal ion complexes²⁸ increase electron-transfer rates, but this is a different case than is being considered here with fluoborate as the counterion. We have attributed⁷ the decrease in reactivity on ion pairing to a decrease in precursor complex stability or an increase in electron-transfer distance, and not merely to a steric effect of blocking part of the reactants surface, since this latter mechanism cannot lead to inhibition by factors of 2 and greater, as has been observed.⁷ Besides the data for this system which are summarized in Table III, inhibition of electron-transfer reactivity upon ion pairing has been observed for the ferrocene self-exchange reaction⁸ and for the reaction between ferrocene and the cobalt clathrochelate mentioned above.⁷

The dependence of the rate constants on solvent can now be considered. It is necessary to first resolve the reaction into the various paths discussed since the contribution of the electrostatic work and that from ion pairing even in the absence of electrostatic work can be large and varies with the solvent. The prediction from Marcus theory⁵ is that the solvent dependence comes from the outer-sphere reorganization while the inner-sphere reorganization that takes place is independent of the solvent. For rate constants that have been corrected for work term effects, like those for paths 1 and 2, or reactions that do not have work terms involved, like paths 5 and 6, the prediction for the dependence of the logarithm of the rate constants on the solvent dielectric parameters is given by eq 12, where n is the index of refraction, r_1 and r_2 are the radii

$$\Delta G^{**} = \Delta G_{\text{out}} + \Delta G_{\text{in}} \quad (12a)$$

$$\Delta G_{\text{out}} = \frac{e^2}{4} \left(\frac{1}{2r_1} + \frac{3}{2r_2} - \frac{1}{R_e} \right) \left(\frac{1}{n^2} - \frac{1}{\epsilon} \right) \quad (12b)$$

$\ln k =$

$$\ln A - \frac{w}{RT} - \frac{\Delta G_{\text{in}}}{RT} - \frac{e^2}{4} \left(\frac{1}{2r_1} + \frac{1}{2r_2} - \frac{1}{R} \right) \left(\frac{1}{n^2} - \frac{1}{\epsilon} \right) \quad (12c)$$

of the reactants, R_e is the distance between the reactant centers in the transition state, and ΔG_{in} is the inner-sphere reorganization energy. Figure 7 shows a plot of the data according to this equation. Path 5 makes the most complete test of the prediction since four of the solvents give values for this rate constant. The fit, like that for the ferrocene exchange and

(28) Endicott, J. F.; Ramasami, T.; Gaswick, D. C.; Tamilarasan, R.; Heeg, M. J.; Brubaker, G. R.; Pyke, S. C. *J. Am. Chem. Soc.* **1983**, *105*, 5301.

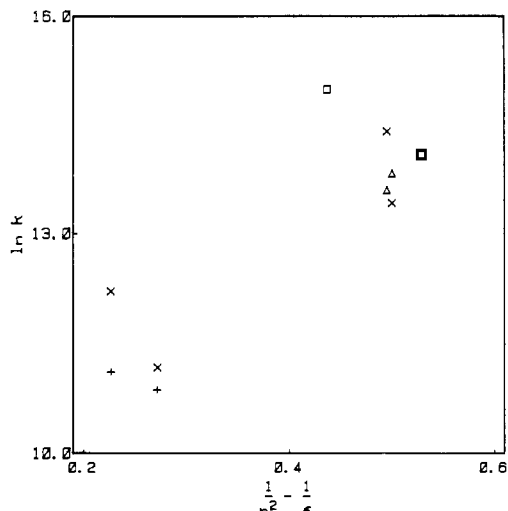


Figure 7. Variation of the rate constant, k , at 26 °C with the dielectric constant term, $1/n^2 - 1/\epsilon$, for the different reaction paths: (□) path 1; (Δ) path 2; (×) path 5; (+) path 6. n is the refractive index and ϵ is the static dielectric constant. Values of n and ϵ are from ref 16. The dielectric constant term for each solvent: $(\text{CH}_3)_2\text{SO}$, 0.4368; CH_3CN , 0.5289; $\text{C}_2\text{H}_5\text{OH}$, 0.5005; $(\text{CH}_3)_2\text{CO}$, 0.4956; $\text{C}_6\text{H}_5\text{Br}$, 0.2273; CHCl_3 , 0.2724.

the ferrocene reduction of the cobalt clathrochelate but unlike the $\text{Cr}(\text{arene})_2^{0/+}$ self-exchange¹⁰ and the $\text{Ru}(\text{hexafluoroacetylacetonate})_3^{0/-}$ self-exchange,⁹ is poor. In the present case the data do not show a good correlation with the solvent parameter. What correlation there is has the wrong sign for the slopes since the theory predicts an increasing rate with decreasing values of $1/n^2 - 1/\epsilon$. Since the theory treats the solvents as a dielectric continuum, the deviation from the prediction is likely to originate in the details of the solvation. This will be a difficult problem to understand, but further experimental results and especially the study of the volumes of activation of the reactions considered here should help define the origins of the deviations.

The activation parameters for the self-exchange in each solvent were measured for the condition of 0.08 M added Bu_4NBF_4 . For the solvents dimethyl sulfoxide and acetonitrile this represents path 1. For bromobenzene and chloroform it represents an average of paths 5 and 6, but primarily path 6. For ethanol this represents paths 2 and 5 and for acetone primarily path 2. We have not studied the temperature dependences of the ion-association constants, but the linearity of the Eyring plots and the concentration dependences, which were also measured at 0.08 M added Bu_4NBF_4 , support the assumption that changes in ion association with temperature are small for all solvents in the presence of 0.08 M added Bu_4NBF_4 . The activation parameters for the more polar solvents dimethyl sulfoxide, acetonitrile, and ethanol show little variation. The decrease in the average rate measured in the

concentration dependences at 0.08 M Bu_4NBF_4 is primarily due to a slightly more negative activation entropy as the solvents become less polar. Chloroform shows a similar entropy of activation as the previous three solvents but a significantly higher activation enthalpy and thus a lower rate constant. Bromobenzene is much different from the other solvents, showing a high activation enthalpy and a more positive activation entropy than any other solvent. This pattern was also observed for the reduction of the cobalt clathrochelate by ferrocene in nitrobenzene.⁷ Within the assumption that the inner-sphere reorganization is constant and thus less than or equal to the observed enthalpy of activation of 3.5 kcal/mol, this increased activation enthalpy must be due to solvation effects with significant enthalpy-entropy compensation. The generally quite negative activation entropies are going to include contributions from the preexponential terms in the rate equation, which in turn reflect the transmission coefficient aspects such as nuclear and electron tunneling and specific orientation requirements.⁴ Since similar activation entropies are measured for ionic and nonionic reactions, path 1 or 2 and path 5 or 6, the negative values of the activation entropy probably have more to do with these preexponential terms than with the charge concentration and increased solvent electrostriction in the transition state.

In conclusion, the electron self-exchange in the $\text{Mn}(\text{CNC}_6\text{H}_{11})_6^{+/2+}$ system has been shown to be sensitive to ion association and the solvent. Ion association generally leads to a decrease in rate constant, after compensation for the electrostatic work required to form the precursor complex. The variation of the solvent changes the rate through changes in ion association and solvation. The solvation contribution is not even qualitatively that predicted by the outer-sphere reorganization term of Marcus' theory. Further work will involve the investigation of the solvation aspects through measurement of volumes of activation²⁹ and study of the effect of changing the size of the complexes.

Acknowledgment. The authors wish to acknowledge the assistance of Professor Don Matteson in initiating this study, of Don Appel with the NMR measurements, and of Dan Borchardt with the electrochemical measurements and for helpful discussions. This work was supported by National Science Foundation Grant CHE-8204-102, by the donors of the Petroleum Research Fund, administered by the American Chemical Society, and by the Boeing Co. through funds for the purchase of the Nicolet NMR.

Registry No. $(\text{C}_6\text{H}_{11}\text{NC})_6\text{MnI}$, 31392-73-1; $(\text{C}_6\text{H}_{11}\text{NC})_6\text{MnBF}_4$, 89463-46-7; $(\text{C}_6\text{H}_{11}\text{NC})_6\text{Mn}(\text{BF}_4)_2$, 89463-47-8.

Supplementary Material Available: Tables of conductivity measurements and ⁵⁵Mn NMR line widths and a conductance vs. concentration plot (10 pages). Ordering information is given on any current masthead page.

(29) Wherland, S. *Inorg. Chem.* **1983**, *22*, 2349.